Volume 3, Number 1, 2026
Pages 1559-1571
Bioscience Insights
ISSN: 3080-3489 (Print)
ISSN: 3080-3497 (Online)
BiosciInsights.com

A NOVEL MULTI-EPITOPE VACCINE AGAINST NIPAH VIRUS USING REVERSE VACCINOLOGY

Wajeha Kamran[*1], Ayesha Tehreem[2], Manahil Khalid[3], Reshyael Irshad Minhas[4], Saba Alamgeer[5], Muhammad Bilal[*6]

*[*1,2,5,6]Institute of Molecular Biology and Biotechnology, Bahauddin Zakariya University, Multan, Pakistan.*
[3]University Institute of Biochemistry and Biotechnology (UIBB), Pir Mehr Ali Shah Arid Agriculture University, Rawalpindi, Pakistan.
[4]National University of Science and Technology (NUST), Islamabad, Pakistan.

[*1]wajehakamran82@gmail.com , [2]ayeshatehreem065@gmail.com ,[3]manahilkhalid179@gmail.com , [4]reshyael17@gmail.com , [5]Sabaalamgeer744@gmail.com , [*6]drbilalmuhammad313@gmail.com

Article Information

Article History

Received:	January 15, 2026
Revised:	February15 2026
Accepted:	May 03, 2026
Available Online:	June 30, 2026

Keywords:

Abstract

Nipah virus (NiV) is a severe pathogen of significant zoonotic potential that causes repeated pandemics of the respiratory system disease and encephalitis, but there is no approved national vaccine against it as of now. This paper has used a reverse vaccinology approach to develop a multi-epitope vaccine against NiV. Viral proteins (nucleoprotein, phosphoprotein, glycoprotein, and matrix protein) were obtained in the UniProt database and filtered with VaxiJen. RANKPEP was used to predict T cell epitopes that had a broad MHC class I and II coverage, and the BepiPred was used to find the linear B-cell epitopes. Appropriate linkers to selected domains were attached, and a chimeric vaccine candidate was formed. The construct was finally shown to be very antigenic, non-allergen, and non-toxic. Analysis showed that the structure was stable, aliphatic index was high, and hydropathicity was almost neutral (GRAVY: -0.065). Secondary structure analysis showed that there were equal proportions of a-helices, b-strands, and coils. AlphaFold prediction and GalaxyRefine refinement yielded a high-quality structure with 98.7% of its residues represented in preferred Ramachandran regions. ClusPro molecular docking depicted positive interactions with HLA molecules and Toll-like receptor 4, and it strongly suggests the activation of adaptive and

innate immune responses. The results suggest that our multi-epitope vaccine is an immunogenic and structurally stable vaccine construct against NiV, which should be further experimentally validated.

Introduction

Nipah virus (NiV) is a new paramyxovirus that is a zoonotic pathogen and was identified in 1998-99 during a fatal outbreak of encephalitis in pig farmers in Malaysia (Spiropoulou 2018). The effects of NiV infection in humans have varied and ranged from asymptomatic carriers to acute respiratory syndrome and lethal encephalitis; in addition, the virus has also repeatedly shown the ability to be transmitted between humans in several outbreaks (Aditi & Shariff 2019). NiV is a species of Nipah henipavirus relating to the subfamily Orthoparamyxovirinae, family Paramyxoviridae, and order Mononegavirales according to the ICTV and related databases (Schoch *et al.* 2020; Walker *et al.* 2022). In the family Henipaviridae, NiV is also one of a number of species, and includes Hendra virus (Hendra henipavirus), Cedar virus, Langya virus, Mojiang virus (MojV), and Ghanaian bat henipavirus (Kumasi virus) (Lefkowitz *et al.* 2017). The first NiV case sprang up after a huge encephalitis outbreak among pig farmers in Malaysia in 1998-9, and it's since shown up again and again as a deadly zoonosis in South and Southeast Asia (Chua 2003). That first Malaysian spillover, in which infected pigs jumped to humans and caused serious disease, economic loss in the swine sector, and high mortality, resulted in NiV becoming a priority for surveillance and research (Epstein *et al.* 2006). Later, the same pattern was repeated in Bangladesh from 2001 onwards and in India at times (including deadly outbreaks in Kerala), and a distinct event with a horse association occurred in the Philippines in 2014 (Ching *et al.* 2015; Yadav *et al.* 2022). Together, they indicate that NiV is not a once-in-a-lifetime local phenomenon but a broader regional danger that does not go away.

NiV infection is clinically characterized by developmental progression of days to neuronal (confusion, disorientation, loss of consciousness) and respiratory symptoms (cough, dyspnea, hypoxia), with increased predisposition to nosocomial and household infection (CDC 2024). Incidents have been reported, most incidents with periods ranging between around 4 and 14 days (with other reported incidences of the protracted disease having a range of 1-40 days), and the clinical progression may lead to coma within 24-48 hours in serious incidences. A series of case early outbreaks and later investigations have consistently documented high ratios of case-fatality, and the survivors have a large proportion reporting long-term neuro/ligand sequelae (Goh *et al.* 2000; WHO 2018). In common with a few other acute viral encephalitis, a unique clinical and virological feature of NiV is the risk of late-onset or reoccurring encephalitis (Alam 2022). A number of follow-up studies and cases, occurring within the Malaysian outbreak, reported decay in neurology in patients, seemingly recovered, weeks to years later; neuropathology examination in such cases has revealed that NiV can substitute itself in foci or remain latent in neural areas, which today can resurrect. The fact that such relapsing cases are less common than acute presentations is worthwhile, as they allow use in long-term efforts to monitor survivors and in regard to vaccine safety issues (Alam 2022; Tan *et al.* 2002).

Currently, no licensed, commercially available human vaccines or universally valid antiviral therapy exists against Nipah virus disease: all current clinical treatment is oppressive, with preclinical or early clinical trials of experimental countermeasures underway. Nipah is a priority pathogen requiring expedited R&D due to its high case-fatality ratio, and bursts of spillover, person-to-person transmission, as well as the technical impediments to wet-lab research that BSL-4 containment requirements may entail, by the World Health Organization and allies (WHO 2018). NIV development of antiviral drugs has so far resulted in few interventions with a consistent response in vivo (Mire *et al.* 2020). The most characterized countermeasure is the humanized monoclonal antibody m102.4 (targeting G attachment glycoprotein, neutralizing both Nipah and Hendra virus) which has proved to be effective post-exposure in several animal models, has been administered on a compassionate-use basis to several potentially high-risk human exposures, and has undergone early-phase safety testing and as a result of this is the present lead candidate as a countermeasure to be used in outbreaks (Zeitlin *et al.* 2024). However, m102.4 is still an unlicensed product, and it has limited access. Other human mAbs are under development and are provisional in animal study, and these include antibodies cross-reacting on F plus G epitopes to henipaviruses (Zeitlin *et al.* 2024).

As NiV is a BSL 4 pathogen in labs, traditional wet-lab vaccine work is expensive and time-consuming, which is the reason why in-silico immunoinformatics approaches are so attractive in terms of being an initial, budget-friendly approach to prioritise vaccine candidates/epitope targets before shifting into the restricted high-containment labs (Mehnaz *et al.* 2024). Having the epitope-based vaccine design methodology to break the complex problem of NiV infection, the most relevant element required of a

vaccine might be the ability to offer protection against the NiV infection (Kaushik 2020). The epitope-based design technique is more careful, efficient, consumes less time, and is non-hazardous, as opposed to the expedient vaccine design technique that is available in trade (Kumar *et al.* 2015). The last vaccine assembly was done by the chosen seven proteins of the NiV. Molecular docking determined immunogenic reactions, three-dimensional (3D) protein modelling to gain a deeper comprehension of the created vaccine candidate, experimentation, and computerized validation and binding strength. Human leukocyte antigens (HLAs) are the most widely used term to refer to the major histocompatibility complex (MHC) alleles in human beings and polymorphic genes (Tong *et al.* 2007). Different studies have shown that the MHC I and II epitopes met the selection and testing potential criteria because they were antigenic (had the ability to induce an immune response), nonallergenic, nontoxic, and different in relation to other human proteins. It was also done with the forecast epitome analysis in case the constructed vaccine would be effective within a heterogeneous population.

Materials and Methods:

The overall workflow employed in this study is illustrated in Figure 1.

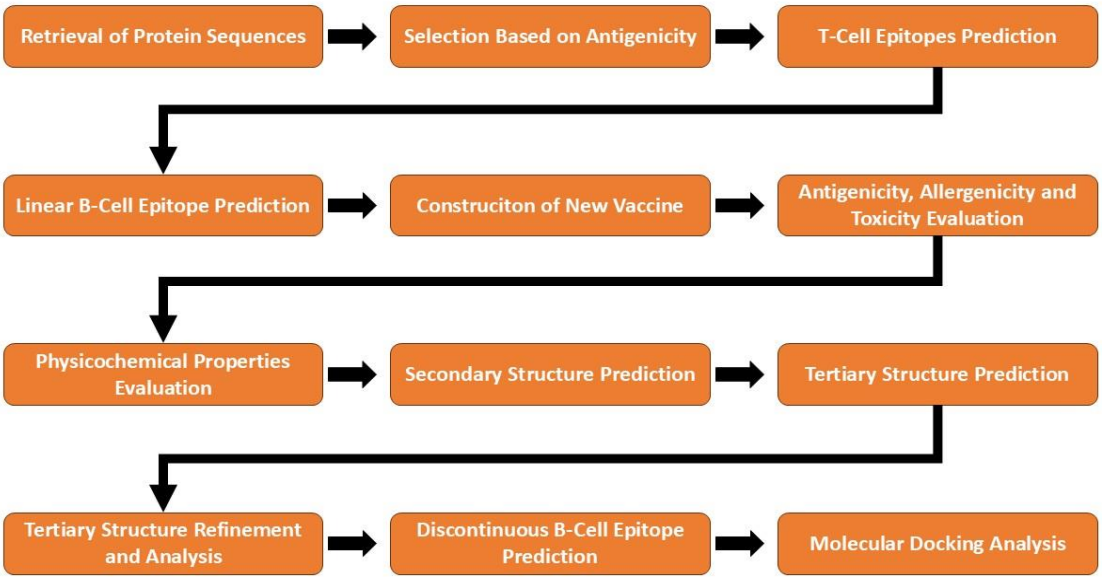


Figure 1: *Methodology employed in this study.*

Obtaining Virus Protein Sequences.

Whole amino-acid sequences of proteins of the NiV were obtained in UniProt Knowledgebase (UniProtKB), a curated and publicly available database that is extensively utilized in the study of immunoinformatics and reverse vaccinology. All the retrieved sequences were checked manually to correct them and to confirm their completeness before assessing them in terms of immunogenicity.

Protein Selection and Immunogenicity Analysis.

Epitope prediction of target proteins was dependent on the initial immunogenicity study to determine the sequences that were likely to elicit the host immune system. To do this, the VaxiJen 3.0 server (https://www.ddg-pharmfac.net/vaxijen3/) was utilized, which is an alignment-independent prediction tool of antigenicity that analyzes proteins in terms of physicochemical characteristics and not through a sequence-based homology (Sotirov & Dimitrov 2024).

Proteins with antigenicity exceeding the required limit were only used in the epitope prediction and vaccine design. These analyses led to the selection of four proteins to be further analyzed for their epitopes: nucleoprotein (Q9IK92), phosphoprotein (Q9IK91), glycoprotein (Q9IH62), and matrix protein (Q9IK90).

T-Cell Epitopes Prediction (HLA Class I and II)

T-cell epitopes with the capacity to attach to human leukocyte antigen (HLA) class I and class II molecules were predicted using the RANKPEP server (http://imed.med.ucm.es/Tools/rankpep.html),

which determines peptide binders using position-specific scoring matrices based on experimentally tested MHC-peptide interactions (Reche *et al.* 2004). The antigenic proteins were furthermore screened based on a representative panel of HLA alleles to cover a wide population. In case of MHC class I, the alleles of HLA-A0201, HLA-A0204, HLA-A0206, HLA-B0702, HLA-B51, HLA-B5301, and HLA-B5401 were incorporated, and the epitope prediction in MHC class II was done through HLA-DRB10101, HLA-DRB10401, HLA-DRB10402, HLA-DRB10701, HLA-DRB10801, HLA-DRB11101, and HLA-DRB11501. Epitopes were selected to include in the multiepitope vaccine construct based on high scores and prediction of binding to several alleles of HLA to increase cellular immune response and population coverage (Kruiswijk *et al.* 2020).

Prediction of Linear B-cell Epitopes

The evaluation of the linear B-cell epitopes was done on the BepiPred 2.0 server (https://tools.iedb.org/bcell), which combines a hidden Markov model and amino acid propensity scales to predict the regions that may be targeted by the B-cell receptors (Jespersen *et al.* 2017). The antigenic proteins of choice were each inputted to the tool of BepiPred, and those with a score over the default cutoff were regarded as potential linear B-cell epitopes.

Multi-epitope Vaccine Construction

After predicting T-cell and B-cell epitopes, the vaccine construct was built based on an epitope-rich domain-based approach instead of building up single short epitopes. Regions that have high antigenicity in every antigenic protein of choice were chosen and harvested as linear B-cell epitopes, HLA class I, and HLA class II containing high-density regions. Such parts with epitopes were then yanked together to create the complete vaccine construct. The separate domains were fused with alanine-based flexible linkers (AAA) to separate the structure of the two domains, minimize the formation of junctional epitopes, and permit the correct presentation of epitopes. To maintain the native epitope context without excessive fragmentation of the antigenic regions to increase the stability and immunogenicity of the generated multi-epitope vaccine, the domain-based methodology was selected.

Antigenicity and Toxicity Evaluation

The designed vaccine construct was tested for its immunological safety and effectiveness by using various in silico prediction tools. VaxiJen v3.0 (https://www.ddg-pharmfac.net/vaxijen3/home) was used to evaluate the total antigenicity potential of the final construct with the help of the viral model and the default threshold value, provided that after domain fusion, the obtained sequence still had a high antigenicity (Sotirov & Dimitrov 2024). To reduce the risk of adverse allergic reactions, the prediction of allergenicity was carried out with the help of AllergenFP (https://ddg-pharmfac.net/AllergenFP/), which considers protein allergenicity as a descriptor-based alignment-free algorithm that groups proteins as either allergenic or non-allergenic based on physicochemical properties (Dimitrov *et al.* 2014). Also, the possible toxicity profile of the vaccine construct was studied with ToxinPred (https://crdd.osdd.net/raghava/toxinpred/), which predicts toxic peptides by amino acid composition and machine-learning algorithms. Constructs that were antigenic, non-allergenic, and non-toxic were only considered in further structural and functional analysis.

Assessment of Physicochemical Parameters

The ExPASy ProtParam (https://web.expasy.org/protparam/) tool was used to analyze the physicochemical properties of the final multi-epitope vaccine construct; it calculates several parameters of the amino acid sequence. Major properties that were considered were the molecular weight, number of atoms, theoretical isoelectric point (pI), instability-index, amino acid composition, aliphatic index, and grand average of hydropathicity (GRAVY). The stability of the protein was predicted using the instability index, which is a value that is lower than the threshold. The aliphatic index was useful to determine the thermostability of the protein, whereas the GRAVY score was obtained to determine hydrophilicity as a whole and solubility. All these parameters provide valuable data on the biochemical behaviour, stability, and appropriateness of the vaccine construct to be later modelled in structure and immunologically tested (Gasteiger *et al.* 2005).

Secondary Structure Prediction

The PSIPRED (https://bioinf.cs.ucl.ac.uk/psipred) and GOR4 (https://npsa-prabi.ibcp.fr/cgi-bin/npsa_automat.pl?page=/NPSA/npsa_gor4.html) servers were used for predicting the secondary structural features of the designed multi-epitope vaccine protein to give an accurate consensus prediction. PSIPRED uses position-specific scoring matrices computed by using PSI-BLAST to

forecast secondary structure elements with a high degree of accuracy, as compared to GOR4, which uses information theory and Bayesian statistics using amino acid sequences (Garnier 1998; McGuffin *et al.* 2000). Both servers were given the vaccine sequence, and the proportions of a-helices, b-strands, and random coils were predicted and analysed. The dual independent prediction methods were used to cross-validate the elements of the secondary structure, which gave a high level of confidence in the structural organization and folding behaviour of the designed vaccine before tertiary-structure-modelling was done.

Tertiary Structure Prediction

AlphaFold (https://alphafoldserver.com), a state-of-the-art protein structure prediction system based on deep learning, was used to predict the three-dimensional (3D) structure of the designed multi-epitope vaccine construct. AlphaFold is a model predicting protein structure by combining all three attributes of the sequence, evolutionary relationship, and physical constraints to create extremely precise structural models (Abramson *et al.* 2024). The complete vaccine sequence was uploaded to the AlphaFold platform, and the most confident model was chosen to undergo more analyses.

Enhancement of the Tertiary Structure.

The previously estimated 3D structure of the multi-epitope vaccine was optimized in GalaxyRefine (https://galaxy.seoklab.org/cgi-bin/submit.cgi?type=REFINE) server, which enhances the quality of the structure by performing repeated repacking of the side chains, and relaxation of the structure (Heo *et al.* 2013). The purpose of the refinement process is to eliminate steric clashes and to increase both the local and global structural stability. After the refinement process, the refined model was tested with the help of several structure validation tools. Stereochemical properties were analyzed by the use of PROCHECK (https://saves.mbi.ucla.edu/) to evaluate the Ramachandran plot, which gives information about the distribution of the residues in the preferred, permitted, and prohibited areas. Also, the overall quality of the protein model was assessed using ERRAT (https://saves.mbi.ucla.edu/) using non-bonded atomic interactions. The use of a combination of these validation tools guaranteed reliability, accuracy, and structural integrity of the refined vaccine model before epitope mapping and docking analyses (Colovos & Yeates 1993; Laskowski *et al.* 1996).

Discontinuous B-Cell Epitopes Prediction.

The ElliPro (https://tools.iedb.org/ellipro/) server was used to predict discontinuous (conformational) B-cell epitopes of the refined multi-epitope vaccine structure, which identifies antibody-accessible epitopes depending on the three-dimensional shape of the protein. ElliPro estimates the shape of the protein to be an ellipsoid and also estimates a protrusion index of each amino acid in the protein, which helps identify regions of the surface exposed to the antibody binding process (Ponomarenko *et al.* 2008). The polished tertiary structure after GalaxyRefine was tried in ElliPro, and predicted conformational epitopes with default parameters were determined. The inferred epitopes were tested to ensure the surface accessibility and spatial distribution of the epitopes of the designed vaccine construct, and this gave more information on the potential of the humoral immune response of the designed vaccine construct.

Molecular Docking Preparation and Analysis

The molecular docking analysis was done to assess the binding affinity and patterns of interaction between the designed multi-epitope vaccine construct and major immune receptors. The optimized three-dimensional structure of the vaccine was docked with Toll-like receptor 4 (TLR4) and the chosen HLA molecules to evaluate the potential of the vaccine to induce innate immune responses as well as adaptive immune responses. The three-dimensional architecture of the immune receptors where docking analysis was conducted was downloaded from the Protein Data Bank (PDB) (https://www.rcsb.org/). The crystal structure of TLR4 was retrieved with accession number *5WJL,* and that of the HLA receptor with accession number *2Z62*. The receptor structures were processed and prepared using UCSF ChimeraX before docking in order to make them compatible with the protein-protein docking conditions (Pettersen *et al.* 2021). The preparation of structures involved the elimination of non-essential components of the structure, including water residues and ligands, and was supplemented by correcting structural irregularities.

Docking simulations were performed with the help of ClusPro server (https://cluspro.org/), which is an automated protein-protein docking system that is used to dock proteins in rigid-body mode, and then known as clustering low-energy conformations (Ashizawa *et al.* 2025). The ligand uploaded was the

vaccine construct, and the receptor structures were downloaded from the Protein Data Bank and acted as docking targets. The resulting docked complexes were ranked by the size of the cluster and the strength of the interaction, and the best docked models were chosen to undergo interaction analysis. The outcomes of these docking experiments were used to obtain knowledge of the structural compatibility and binding stability of the vaccine candidate with immune receptors, and provided evidence in favour of its possible immunogenic efficacy.

Results

Selection of Immunogenic Proteins:

The antigenic potential of all the structural and accessory proteins of NiV stored at UniProt was first filtered in the VaxiJen v3.0 server. This analysis showed that four proteins, the nucleoprotein, phosphoprotein, glycoprotein, and the matrix protein, had 100 percent probability of being immunogenic, which implies that there are high chances of the protein triggering host immune responses. On the basis of these results, the Nucleoprotein (Q9IK92), Phosphoprotein (Q9IK91), Glycoprotein (Q9IH62), and matrix protein (Q9IK90) were chosen to be downstreamly predicted and used to design vaccines. These proteins are significant in the viral replication, assembly, host cell entry, and immune recognition, hence making them good targets of a multi-epitope vaccine approach. The selected immunogenic proteins and their characteristics are summarized in Table 1.

Table 1: *List of proteins that were used to construct a multi-epitope vaccine.*

Protein Name	UniProt Accession Number	Function	Vaxijen 3.0 Results
Nucleoprotein	Q9IK92	Encapsulates the viral RNA genome and plays a central role in viral transcription and replication by forming the ribonucleoprotein complex.	100% Probable Immunogen
Phosphoprotein	Q9IK91	Acts as a cofactor for the viral RNA-dependent RNA polymerase and is essential for viral RNA synthesis and replication.	100% Probable Immunogen
Glycoprotein	Q9IH62	Mediates viral attachment and entry into host cells by binding to cellular receptors, making it a primary target for neutralizing antibodies.	100% Probable Immunogen
Matrix Protein	Q9IK90	Facilitates viral assembly and budding by linking the viral nucleocapsid to the host cell membrane during virion formation.	100% Probable Immunogen

T-cell Epitope Prediction (MHC Class I & II):

Predicted MHC class I epitopes are presented in Table 2.

Table 2: *Predicted MHC Class I T-Cell Epitopes*

Antigen	HLA_A0 201	HLA_A0 204	HLA_A0 206	HLA_B0 702	HLA_B 51	HLA_B 5401	HLA_B 5301
Nucleoprotein	296-304 SLMLLY REI 283-291 ALNEFQ SDL 329-337 LLWSFA MGV	329-337 LLWSFA MGV 354-362 YLEPMY FRL		305-313 GPRAP YMVL	327-335 YPLLW SFAM 279-287 YPALA LNEF 305-313 GPRAP YMVL		
Phosphoprotein	516-524 VLMGVI NSI 545-553	106-114 QLDPVV TDV	516-524 VLMGV INSI	396-404 MPKSR GIPI	396-404 MPKSR GIPI 394-402	396-404 MPKSR GIPI	

	KIINKLESI				TPMPKSRGI		
Glycoprotein	55-63 ALLGSIVII 62-70 IIVMNIMII		587-595 VIRPKLFAV 55-63 ALLGSIVII	589-596 RPKLFAVKI	589-596 RPKLFAVKI		
Matrix Protein	231-239 KVASFMLHL 270-278 SIGGLSLHI	235-243 FMLHLGNFV	270-278 SIGGLSLHI		102-110 HPQDLLEEL	92-100 YPLGVGKSA	102-110 HPQDLLEEL

Predicted MHC class II epitopes are shown in Table 3.

Table 3: *Predicted MHC Class II T-Cell Epitopes*

Antigen	HLA-DRB10101	HLA-DRB10401	HLA-DRB10402	HLA-DRB10701	HLA-DRB10801	HLA-DRB11101	HLA-DRB11501
Nucleoprotein	327-335 YPLLWSFAM	273-281 FGLETRYPA		327-335 YPLLWSFAM		327-335 YPLLWSFAM	298-306 MLLYREIGP 284-292 LNEFQSDLN
Phosphoprotein			529-537 LDMRLNHIE 543-551 IPKIINKLE		541-549 KEIPKIINK	393-401 GTPMPKSRG	
Glycoprotein	67-75 IMIIQNYTR 547-555 YRAQLASED	547-555 YRAQLASED 551-559 LASEDTNAQ	545-553 ILYRAQLAS	566-574 FLLKNKIWC	537-545 FTVFKDNEI		533-541 ENPVFTVFK
Matrix Protein	86-94 IRTIAAYPL 92-100 YPLGVGKSA	231-239 KVASFMLHL 96-104 VGKSASHPQ	262-270 MKLQFSLGS			239-247 MKLQFSLGS 232-240 VASFMLHLG	243-251 VRRAGKYYS 236-244 MLHLGNFVR

This was done by prediction of T-cell epitopes of proteins of NiV using the RANKPEP server, which helps in identifying peptides that can bind MHC class I and MHC class II molecules. Several alleles of HLA class I and class II were examined to have a wide population coverage. The results of the analysis revealed that there were a lot of high-affinity binding epitopes in all four chosen proteins and that there were overlapping regions of MHC class I and class II binding potential. The prediction of the epitopes was identified as found all across the protein sequences, suggesting that the protein contains numerous immunogenic regions that can induce the occurrence of cytotoxic and helper T-cell responses. The

epitopes were then identified, and the domains containing the epitopes were delimited to include in the multi-epitope vaccine construct.

Linear B-Cell Epitope:

The BepiPred 2.0 server was used to predict amino acid regions with the greatest potential to be antigenically recognized by a B-cell, and thus, linear B-cell epitope prediction of the selected antigenic proteins was conducted. The analysis has shown that there are several linear B-cell epitopes in all four proteins, with several regions having high prediction scores at all above the threshold value. The availability of various high-scoring linear B-cell epitopes on several proteins that are selected to be included in the vaccine design justifies their appropriateness in the vaccine design. The predicted epitopes were once more utilized in determining epitope-rich domains to be incorporated in the multi-epitope vaccine construct. The predicted linear B-cell epitopes are summarized in Table 4.

Table 4: *Linear B-cell epitopes predicted by the BepiPred 2.0 for the selected proteins*

Protein	No.	Start	End	Peptide	Length
Nucleoprotein	1	6	29	EEAASFRSYQSKLGRDGRASAATA	24
	2	44	46	SPE	3
	3	92	95	LNDP	4
	4	109	130	NGIPVMERRGDKAQEEMEGLMR	22
	5	133	158	KTARDSSKGKTPFVDSRAYGLRITDM	26
	6	184	216	DTAEESETRRWAKYVQQKRVNPFFALTQQW LTE	33
	7	240	247	KGGSAKGR	8
	8	292	292	N	1
	9	303	303	E	1
	10	305	305	G	1
	11	318	323	IQTKFA	6
	12	343	355	RSMGALNINRGYL	13
	13	368	377	RHHAGGIDQN	10
	14	379	381	ANR	3
	15	383	390	GLSSDQVA	8
	16	398	474	ETSAGRQESNVQAREAKFAAGGVLIGGSDQD IDEGEEPIEQSGRQSVTFKREMSISSLANSVPSS SVSTSGGTRLTN	77
	17	477	477	L	1
	18	487	528	AAKEAASSNATDDPAISNRTQGESEKKNNQD LKPAQNDLDFV	42
Phosphoprotein	1	22	107	KEIQKTYGRSSIQQPSIKDQTKAWEDFLQCTS GESEQVEGGMSKDDGDVERRNLEDLSSTSPT DGTIGKRVSNTRDWAEGSDDIQL	86
	2	120	146	GGECTGYGFTSSPERGWSDYTSGANNG	27
	3	155	233	KMLSYAPEIAVSKEDRETDLVHLENKLSTTGL NPTAVPFTLRNLSDPAKDSPVIAEHYYGLGVK EQNVGPQTSRNVNLD	79
	4	238	258	YTSDDEEADQLEFEDEFAGSS	21

	5	267	340	PEDEEPSSVGGKPNESIGRTIEGQSIRDNLQAK DNKSTDVPGAGPKDSAVKEEPPQKRLPMLAE EFECSGSEDP	74
	6	347	515	KENSLINCQQGKDAQPPYHWSIERSISPDKTEI VNGAVQTADRQRPGTPMPKSRGIPIKKGTDA KYPSAGTENVPGSKSGATRHVRGSPPYQEGK SVNAENVQLNASTAVKETDKSEVNPVDDNDS LDDKYIMPSDDFSNTFFPHDTDRLNYHADHL GDYDLETLCEES	169
	7	526	526	L	1
	8	528	531	NLDM	4
	9	538	538	E	1
	10	541	541	K	1
	11	545	545	K	1
	12	552	552	S	1
	13	555	556	RV	2
	14	558	558	A	1
	15	582	659	GKGERKGKNNPELKPVIGRDILEQQSLFSFDN VKNFRDGSLTNEPYGAAVQLREDLILPELNFE ETNASQFVPMADDS	78
	16	671	679	HIKDRELRS	9
	17	689	696	ENDEEIQE	8
Glycoprotein	1	8	43	VRFENTTSDKGKIPSKVIKSYYGTMDIKKINE GLLD	36
	2	75	82	RSTDNQAV	8
	3	91	92	QQ	2
	4	95	99	KGLAD	5
	5	102	102	G	1
	6	110	110	S	1
	7	137	137	S	1
	8	139	214	NENVNEKCKFTLPPLKIHECNISCPNPLPFREY RPQTEGVSNLVGLPNNICLQKTSNQILKPKLIS YTLPVVGQSG	76
	9	239	245	SCSRGVS	7
	10	260	262	DEV	3
	11	273	277	PPNPN	5
	12	300	313	VGDPILNSTYWSGS	14
	13	325	343	SNGGGYNQHQLALRSIEKG	19
	14	371	405	VRTEFKYNDSNCPITKCQYSKPENCRLSMGIR PNS	35
	15	433	433	D	1
	16	460	462	WDT	3

	17	483	498	TVISRPGQSQCPRFNT	16
	18	530	532	QTA	3
	19	553	558	SEDTNA	6
Matrix protein	1	5	41	IKSISSESMEGVSDFSPSSWEHGGYLDKVEPEI DENG	37
	2	51	59	TPGANERKY	9
	3	74	84	VERTPETGKRK	11
	4	98	106	KSASHPQDL	9
	5	108	108	E	1
	6	122	123	GS	2
	7	134	146	PLNHLVPWKKVLT	13
	8	158	166	RNVDQIQLD	9
	9	185	186	GI	2
	10	214	229	ADLSKMGIQGSLDKDG	16
	11	245	254	RAGKYYSVDY	10
	12	293	293	G	1
	13	330	337	SIPREFMI	8
	14	343	349	IDNTGRI	7

The Multi-epitope Vaccine Construction:

The selection of NiV proteins was done based on the predicted T cell and B cell epitopes, and the generated epitope-rich regions were used in the construction of the multiepitope vaccine candidate. To maintain the context of an epitope and structural continuity of proteins, continuous domains with a high concentration of overlapping MHC class I, MHC class II, and linear B-cell epitopes were isolated per protein, rather than collecting the individual epitopes. These domains, characterized by epitopes, were based on the nucleoprotein, phosphoprotein, glycoprotein, and matrix protein, and they were sequentially conjugated to produce one chimeric vaccine construct. The domains were joined with flexible alanine-based linkers (AAA), which enabled these domains to be folded independently and minimise chances of steric hindrance between the adjacent sections. The final vaccine construct was a single poly peptide sequence with a multiplicity of immunogenic regions, which was aimed at producing a cellular and humoral immune response.

Assessment of Antigenicity, Allergenicity, and Toxicity:

The last multi-epitope vaccine construct was tested in terms of antigenic potential, allergenicity, and toxicity using known in silico prediction tools. The antigenicity test conducted on the VaxiJen v3.0 server indicated that the vaccine construct was 100% probable antigen, which means that it is likely to induce an immune response. The analysis of the construct using AllergenFP predicted that the construct is non-allergenic, indicating a low probability of causing allergic reactions. Also, toxicity prediction done by using the ToxinPred server demonstrated that the vaccine sequence is non-toxic, which confirms the safety of the vaccine at the peptide level. All these findings would suggest that the constructed multi-epitope vaccine has positive immunogenic and safety features, which would justify its applicability in further structure and interaction studies. The detailed evaluation results are presented in Table 5.

Table 5: *Antigenicity, allergenicity, and toxicity evaluation results.*

Antigenicity	**VaxiJen 3.0**	Probable antigen (100%)
	ANTIGENpro	Probable antigen (0.61)
Allergenicity	**AllergenFP 1.0**	Probable non-allergen

Toxicity	**ToxinPred**	Non-toxic

1.6. Physicochemical Parameters Evaluation:

Physicochemical characteristics and stability of the final multi-epitope vaccine construct were assessed with the help of ExPASy ProtParam depository to determine biochemical properties of the vaccine construct. The constructed protein vaccine was made of 401 amino acids and had a calculated molecular weight of 44.55 kDa and a theoretical isoelectric point (pI) of 8.71, which corresponds to a basic protein. Charged residue analysis revealed that positively charged residues (Arg + Lys: 47) were a little more than the negatively charged ones (Asp + Glu: 43). The instability index was determined as 32.52, which categorizes the protein as being stable. The aliphatic index of 98.85 implied a high level of thermostability, whereas the GRAVY value of 0.065 implied a general hydrophilic nature, which is positive in terms of solubility. Also, it was estimated that the half-life of the construct in *Escherichia coli* should be over 10 hours, whereas in yeast and mammalian cells, it should be over 20 and 30 hours, respectively, which positively indicated the possibility of the vaccine protein being employed in downstream applications and expression. The physicochemical characteristics of the final vaccine construct are summarized in Table 6.

Table 6*: Results of physicochemical parameters from ProtParam*

Parameter	Value
Amino acids	401
Molecular weight	44550.65 Da
Theoretical pI	8.71
Instability index	32.52
Aliphatic index	98.85
GRAVY	-0.065
Estimated half-life	30 h (mammalian, in vitro)
Total number of atoms	6340

1.7. Secondary Structure Prediction:

PSIPRED and GOR4 servers were used to predict the folding properties of the multi-epitope vaccine construct by calculating the secondary structural composition of the vaccine construct. Analysis of PSIPRED indicated that the vaccine sequence was made up of a- helices and random coils mostly, with b- strand regions scattered throughout the sequence. The graphical depiction reported a well-structured organization with no massive areas of disorganization. The secondary structure elements were also measured by complementary analysis with the GOR4 server, revealing that 48.13% (193 residues) of the entire sequence were a-helices, and 17.96% (72 residues) of the entire sequence were extended b-strands. Random coils composed 33.92 percent (136 residues) of the structure. No p-helices, 310-helices, b-turns, or ambiguous states were anticipated. The sum of both instruments revealed a structurally diverse and stable structure of secondary structure, which is appropriate to use to model the tertiary structure. The PSIPRED secondary structure prediction is shown in Figure 2 and also the GOR4 secondary structure prediction is presented in Figure 3 below figure 2.

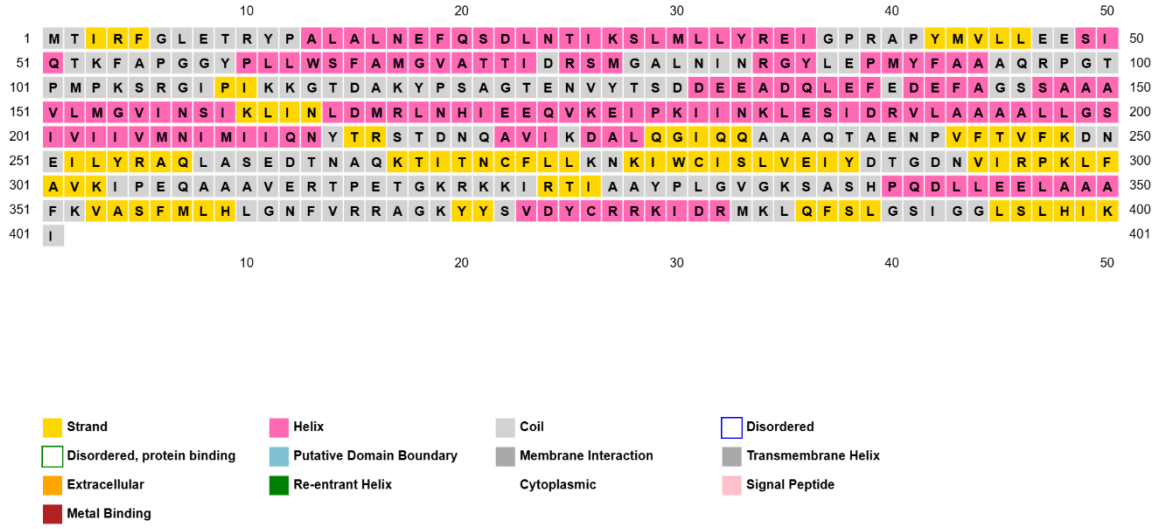


Figure 2: *Secondary structure prediction results from PsiPred.*

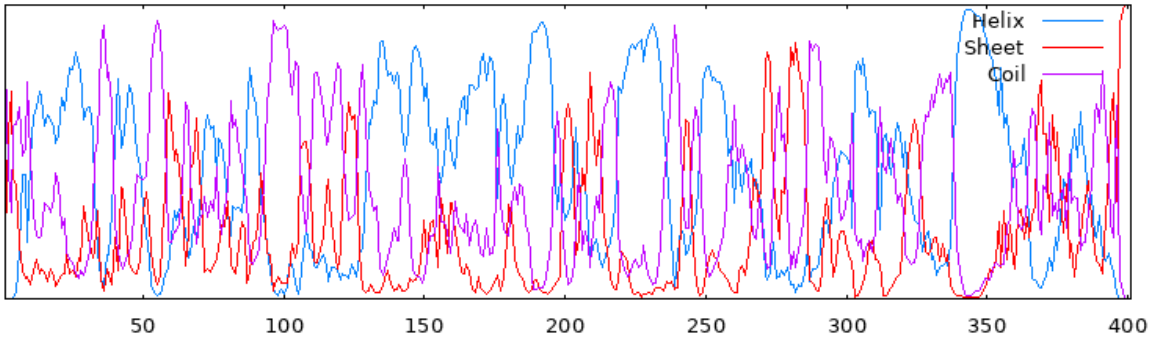


Figure 3: *Secondary structure prediction results from GOR4*

Tertiary Structure Prediction, Refinement, and Validation

The AlphaFold protein structure prediction system was used to predict the three-dimensional structure of the designed multi-epitope vaccine construct. Structural models were produced in the selected AlphaFold model is shown in Figure 4 where the full length of the vaccine sequence (five structural models), representing a possible folding conformation. One of them, the most structured AlphaFold model, was chosen for further analysis due to its general completeness and consistency of structure. The chosen model exhibited a small and well-structured architecture; the a- helical and b-strand elements were positionally organized in relation to the expected secondary structure. The fact that no major structural discontinuities were suggested indicated that the multi-domain construct was properly folded. Subsequent refinements, validation, conformational epitope prediction, as well as molecular docking studies were done on the basis of this predicted tertiary structure.



Figure 4: *Ranked 1 tertiary structure predicted by the AlphaFold*

The tertiary structure of the multi-epitope vaccine, as initially predicted, was refined on the GalaxyRefine server, which created five refined structural models. The GDT-HA and RMSD comparison of the refined models is shown in Figure 5.. Comparison of refinement parameters has shown that the structural quality has greatly improved in all the refined models as compared to the original structure. Model 2 was chosen among the generated models as the final refined structure with a positive balance between structural accuracy and stereochemical quality. Model 2 had a GDT-HA score of 0.8853 and an RMSD of 0.584Å, which showed that there was very minimal deviation of the initial model, whereas the refinement was better. The MolProbity score had reduced to 1.258 (final) compared to 1.966, indicating superior quality of the entire structure are presented in Figure 6. Besides, Model 2 showed a smaller clash score (4.9) and a significantly lower percentage of poor rotamers (0.3%). Ramachandran plot analysis showed a considerable number of residues present in the preferred regions, which has been increasing from 85.2 percent in the first model to 98.7 percent in the second Model 2. Clash score and Ramachandran favored residues are shown in Figure 7

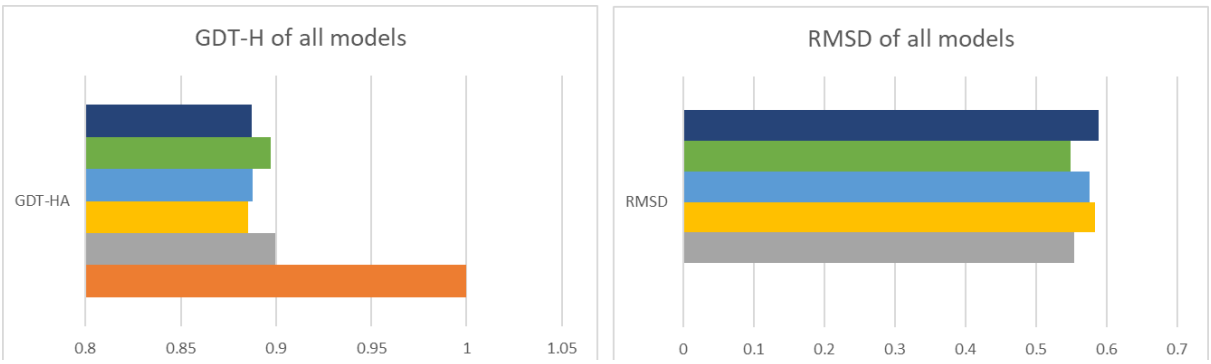


Figure 5: *GDT-H (left) and RMSD (right) of initial and 5 refined from GalaxyRefine*

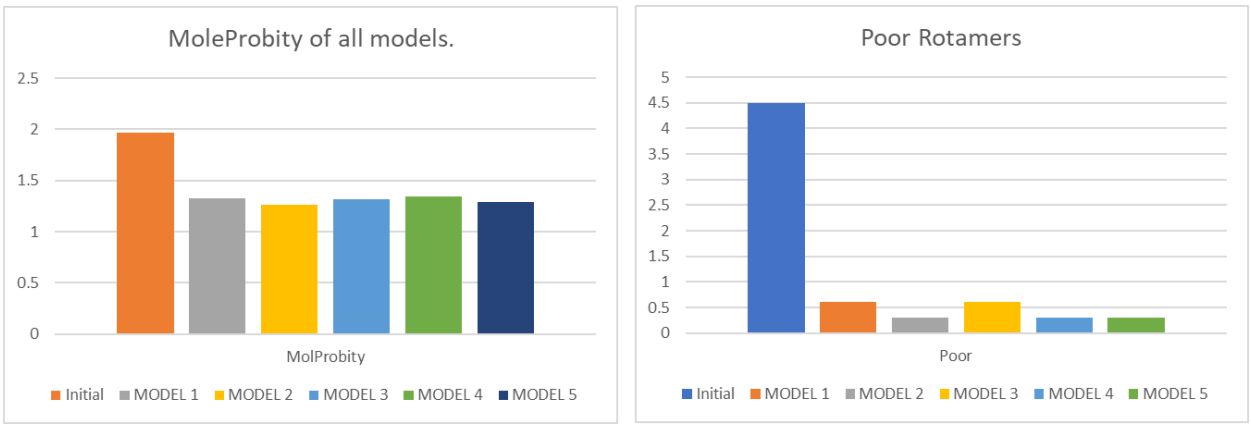


Figure 6: *MoleProbity (left) and Poor rotamers (right) values of initial and 5 refined models from GalaxyRefine*

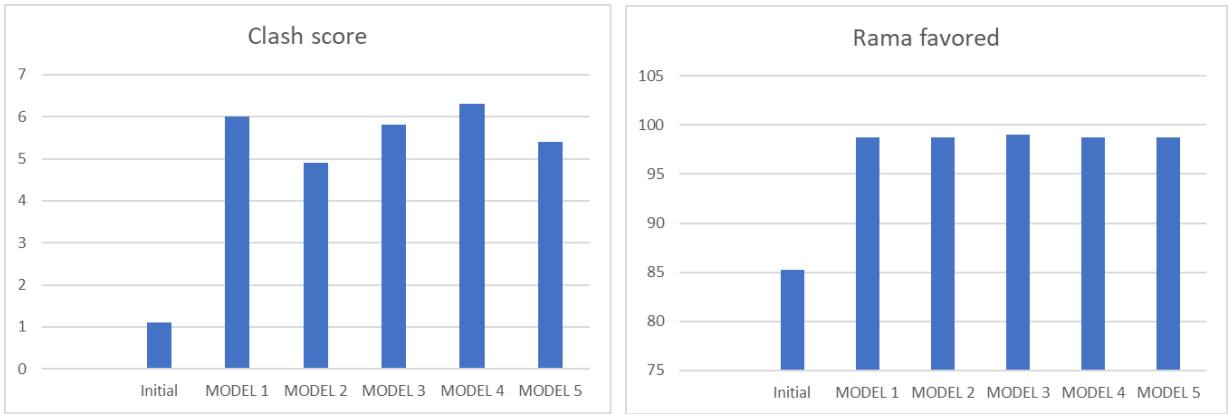


Figure 7: *Clash score (left) and Rama favored (right) of initial and 5 refined models from GalaxyRefine*

The superimposition of the initial and refined structures is illustrated in Figure 8.

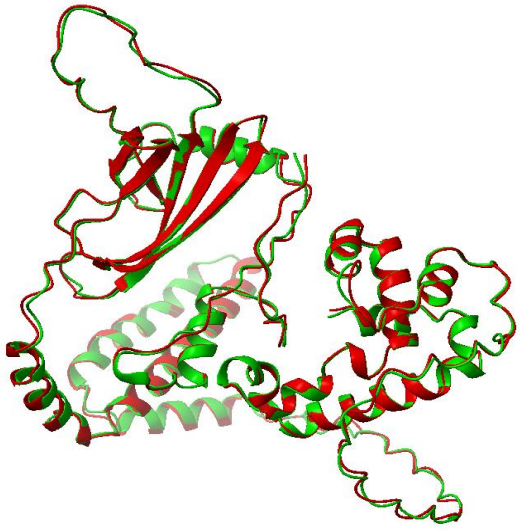


Figure 8: *Before and after refinement models superimposed on each other; red=initial; green=refined Model2*

Structural integrity was further checked on ProSA-web and ERRAT. ProSA-web analysis revealed an increase in the Z-score, from -3.98 of the first structure to -4.69 of Model 2, which reflects the improved model reliability in the range used to compare experimental structures of protein. These findings were substantiated by ERRAT analysis, and the overall quality factor rose to 88 by refinement as compared to 84. All these validation findings confirmed that Model 2 was the most valid and structurally optimized model to be used in downstream epitope mapping and molecular docking studies.

ProCheck was employed to visualize Ramachandran plots for initial and refined 3D models. These plots help us visualize the residues in Rama-favoured, allowed, and disallowed regions. The red regions in the plots account for the favoured region, the shades of yellow account for additionally and generously

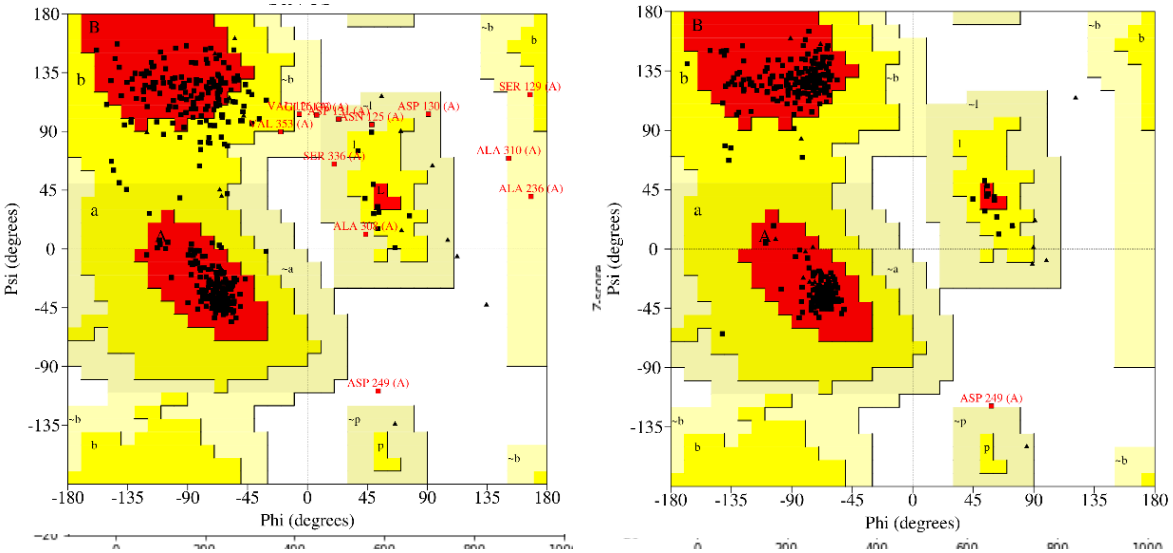


Figure 9: *Ramachandaran plots obtained from ProCheck showing residues in Rama-favoured, allowed and disallowed regions.*

allowed regions, and the white areas indicate the disallowed region. Results show that while most of the residues were already in the favoured and allowed regions, the number of residues in the favoured regions significantly increased following the refinement. The Ramachandran plots are presented in Figure 9.

Prediction of Discontinuous B-Cell Epitopes

The multi-epitope vaccine construct of three refined three-dimensional structures was analyzed by ElliPro server to predict discontinuous (conformational) B-cell epitopes. ElliPro selected several conformational epitopes scattered across the surface of the vaccine protein, which shows that there are regions available to the antibody. The proposed epitopes had a minimum Protrusion index score of 0.537 with a maximum score of 0.939, indicating a difference in the intensity of surface exposure and structure prominence. Protein structure regions that were the most exposed scored higher in the epitopes, whereas moderately exposed conformational regions were reported as the lower-scoring epitopes. The B-cell epitopes of the designed vaccine construct were also predicted discontinuously, which also supports the potential of the vaccine construct in eliciting effective humoral immune responses. The predicted discontinuous B-cell epitopes are summarized in Table 8, while the two highest-scoring discontinuous B-cell epitopes are illustrated in Figure 10.

Table 7: *List of discontinuous B-cell epitopes predicted by the ElliPro server.*

No.	Residues	Number of residues	Score
1	A:T128, A:S129, A:D130, A:D131, A:E132	5	0.939
2	A:Q307, A:A308, A:A309, A:A310, A:V311, A:E312, A:R313, A:T314, A:P315, A:E316, A:T317, A:G318, A:K319, A:K321, A:K322, A:I323	16	0.903

3	A:K112, A:G113, A:T114, A:D115, A:A116, A:K117, A:Y118, A:P119, A:S120, A:A121, A:G122, A:T123, A:E124, A:N125, A:V126, A:Y127	16	0.875
4	A:R106, A:G107, A:I108, A:P109, A:I110	5	0.873
5	A:A144, A:G145, A:S146, A:S147, A:A148, A:A149, A:A150, A:V151, A:L152, A:M153, A:G154, A:V155, A:I156, A:N157, A:S158, A:I159, A:K160, A:L161, A:I162, A:N163, A:L164, A:D165, A:M166, A:R167, A:L168, A:N169, A:H170, A:I171, A:E172, A:E173, A:Q174, A:V175, A:K176, A:E177, A:I178, A:P179, A:K180, A:I181, A:I182, A:N183, A:K184, A:L185, A:E186, A:S187, A:I188, A:D189, A:R190, A:V191, A:L192, A:A193, A:A194, A:A195, A:A196, A:L197, A:L198, A:I201	56	0.803
6	A:E133, A:A134, A:D135, A:Q136, A:L137, A:E138	6	0.796
7	A:F139, A:E140, A:D141, A:E142, A:F143	5	0.693
8	A:A93, A:A94, A:Q96, A:R97, A:P98, A:G99, A:T100, A:P101	8	0.675
9	A:V246, A:F247, A:K248, A:D249, A:N250, A:E251, A:I252, A:L253, A:Y254, A:R324	10	0.66
10	A:S217, A:T218, A:D219, A:N220, A:Q221, A:A222, A:V223, A:I224, A:K225, A:D226, A:A227, A:L228, A:Q229, A:G230, A:I231, A:Q232, A:Q233, A:A234, A:A235, A:A236, A:Q237, A:T238, A:A239, A:E240, A:N241, A:D262, A:T263	27	0.651
11	A:T9, A:Y11, A:P12, A:A13, A:L14, A:A15, A:L16, A:N17, A:E18, A:F19	10	0.593
12	A:K276, A:N277, A:K278, A:P305, A:E306	5	0.59
13	A:L87, A:E88, A:P89, A:M90, A:Y91, A:M102, A:P103	7	0.583
14	A:K335, A:S336, A:A337, A:S338, A:H339, A:P340, A:Q341, A:D342	8	0.576
15	A:Q20, A:S21, A:N24	3	0.555
16	A:V205, A:I208, A:Q212, A:T215, A:R216	5	0.548
17	A:T325, A:I326, A:A327	3	0.537

1.10. Molecular docking analysis.

The molecular docking analysis was conducted on the ClusPro server to determine the potential of the refined multi-epitope vaccine construct to interact with the immune receptor, such as HLA molecules and TLR4. Docking simulations were done in Balanced mode, which combines terms of van der Waals, electrostatic interaction, and the desolvation energy to find biologically interesting protein-protein interactions.

In the case of HLA receptor docking, a set of docking complexes was generated and clustered in terms of structural similarity and energy of interaction. The clusters that resulted had good binding affinity with weighted scores of: -891.5 to -1247.5. A number of groups displayed very desirable interaction energies, and the very lowest energy values were -1247.5, which showed that there was a binding that was stable between the vaccine construct and the HLA molecules. The fact that there were large cluster sizes also indicated that binding orientations were consistent and reproducible between a number of docking poses.

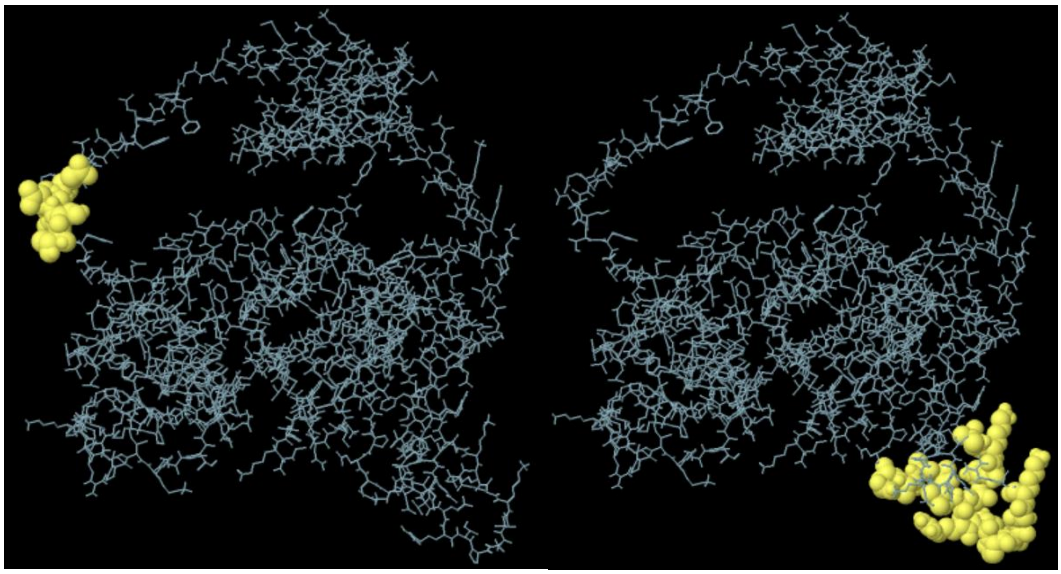


Figure 10: *Two highest scoring predicted discontinuous B-cell epitopes with values of 0.939 (left) and 0.903 (left) respectively.*

A number of energetically favourable complexes were also obtained by docking with TLR4. The weights of the scores of the TLR4 docking clusters are -0.765.5 to -1091.7, with the minimum energy values at -1145.2. There were a few clusters that had a large number of interactions, implying that there were stable and repetitive patterns of interaction between the vaccine construct and TLR4. All the above results indicate that the designed vaccine strongly binds to the antigen-presenting and innate immune receptors and can be used to induce both adaptive and innate immune responses. The best docked complexes of the vaccine construct with HLA and TLR4 receptors are shown in Figure 11.

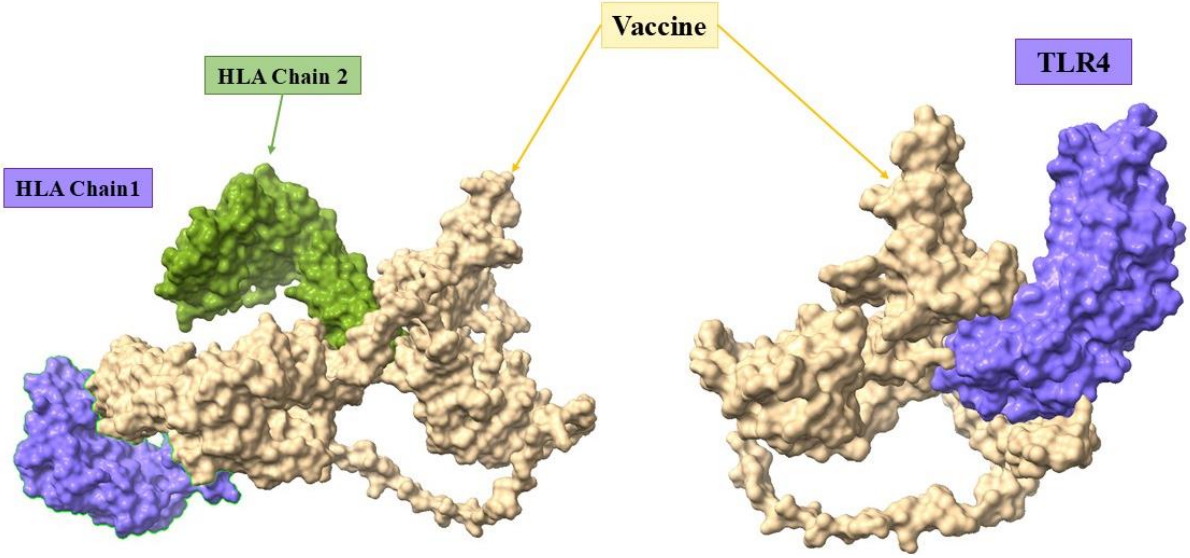


Figure 11*: 3D representation of top-ranking docked model for each receptor; with HLA (left) and with TLR4(right)*

Results Discussion

NiV is still a severe zoonotic agent whose case fatality rate is high, and no approved human vaccine is available, which is why it is crucial to develop practical preventive methods (Chan *et al.* 2025). The current project utilized an immunoinformatics-based, entirely in silico method of designing a multi-epitope vaccine candidate against NiV, incorporating screening of antigenicity, epitope prediction, structural modeling, and receptor docking (Kaushik 2020). The rationale behind this approach was to address constraints linked with the traditional vaccine development process, namely, expensive

development and a lengthy development cycle, and biosafety issues linked with work with dangerous pathogens like NiV.

A major strength of this study is that the selection of viral proteins was rational, having been selected according to antigenicity analysis. Nucleoprotein, phosphoprotein, glycoprotein, and matrix proteins of the Nipah virus were found to be the most immunogenic proteins with 100 percent probability of antigenicity, as indicated by the VaxiJen server (Sotirov & Dimitrov 2024). These proteins are unique and vital functional units of the viral life cycle, which, together, encompass viral accessibility, multiplication, transcription, and assembly.

This study also compared with many traditional designs of multi-epitope vaccines, which involve assembling short, single epitopes, whereas the design of this study was an epitope-rich domain-based design, whereby contiguous protein sub-regions with overlapping T-cell and B-cell epitopes were picked. Such a design option maintains the natural sequence context of epitopes, which may enhance antigen processing, MHC presentation, and immune recognition (Enayatkhani *et al.* 2021). The sampling of various groups of HLA class I (HLA- A0201, A0204, A0206, B0702, B51, B5301, B5401) and class II (HLA-DRB1*0101, *0401, *0402, *0701, *0801, *1101, *1501) was attempted to reflect a global representation of HLA. This is significant as HLA allele frequencies have varied significantly between human populations, and high coverage of the population is an advantageous characteristic of universal vaccine candidates. The integration of multi-epitope designs that bind several different HLA alleles has been demonstrated to enhance theoretical population coverage and immune response so that potential disparities in vaccine efficacy among different ethnic and geographical backgrounds may be minimized.

Besides cellular immunity, humoral immune responses were supported with linear B-cell epitopes that were identified with the help of the BepiPred algorithm. Production of antibodies involves B-cell epitopes and is essential in overcoming extracellular pathogens and preventing the entry of viruses into host cells. Other past research studies on Nipah virus immunoinformatics vaccine design have also integrated B-cell prediction to select surface-accessible areas that can be used to produce antibodies that prevent the process of virus attachment or fusion.

Flexible alanine-based (AAA) linkers are also used so as to facilitate proper separation of domains and to reduce steric interference and junctional epitope formation. This method has also led to a better structural stability that can be seen in the positive physicochemical characteristics of the end construct. The antigenicity, allergenicity, and toxicity were all evidence that the vaccine construct that was designed has a high immunogenicity profile but has an acceptable safety profile. Its theoretical appropriateness for further development is supported by the fact that the construct is classified as antigenic, non-allergenic, and non-toxic.

Prediction of tertiary structure with AlphaFold gave a high-quality structural model of the vaccine construct, and the three-dimensional architecture was shown to be compact and organized. AlphaFold is demonstrated to be more accurate than other homology-based protein modeling systems, especially in the case of chimeric or novel protein constructs without any close structural template (Jumper et al., 2021). A top-ranked AlphaFold model was selected to make sure that the most structurally consistent version was used in the further refinement and docking analyses. The fact that there were no key disordered regions or steric clashes in the predicted model indicated that the epitope-rich domains and linker regions were capable of being compatible with stable folding.

High-quality identification and selection of immunogenic peptide regions that bind to TLR and HLA molecules and result in effective cellular and humoral immune responses are critical factors that determine the success of an epitope-based vaccine. Additionally, our designed vaccine candidate met all selection criteria to come up with an appropriate vaccine. The resultant vaccine created is 401 amino acid residues. Molecular docking analysis in this study has been done to determine the binding compatibility of the designed multi-epitope vaccine construct with Toll-like receptor 4 (TLR4) and HLA molecules, which are key elements of the innate immune sensing and the antigen presentation pathways, respectively. The binding interactions obtained with the ClusPro server under docking simulations showed a good and consistent binding interaction, as indicated by high weighted scores and low energy values of the various clusters. There was a stable complex between the NiV and TLR4 and HLA receptors. The molecular docking results showed that the developed vaccine binds effectively with the TLR molecule with a weighted score of -917.9 with 64 members in Model-0 and with the

lowest weighted score of -942.5 with 62 members in Model-1. The resulting multiepitope NiV vaccine is very immunogenic, safe, and nontoxic, according to our computational research findings. These results clearly show that the immunogen employed in this study was competent to induce antibody formation in vivo.

Conclusion

The current paper has utilized a multi-epitope vaccine candidate design and evaluation with the help of a thorough immunoinformatics-based analysis, working with the free and open-source possibilities to design vaccines. All of the performed computational analyses suggest that our designed vaccine can be a strong candidate for protecting against NiV. Even though the conclusions of the present study are made on the basis of computational predictions, which need to be confirmed by experimental research, all the results obtained point to the fact that the developed multi-epitope vaccine candidate is an effective prophylactic measure against the Nipah virus infection.

Acknowledgement

Author acknowledgment goes here.

Conflict of Interest:

The authors declared that there is no conflict of interests.

Ethical Statement:

In this research, no living being is used for experimental purpose.

Supplementary Data

Table 8: *Table of results for docking with TLR receptor*

Cluster	Members	Representative	Weighted Score
0	64	Center	-910.7
		Lowest Energy	-917.9
1	62	Center	-798.4
		Lowest Energy	-942.5
2	52	Center	-845.9
		Lowest Energy	-892.1
3	48	Center	-851.1
		Lowest Energy	-1022.5
4	46	Center	-893.7
		Lowest Energy	-963.3
5	35	Center	-913.8
		Lowest Energy	-1145.2
6	35	Center	-1091.7
		Lowest Energy	-1091.7
7	30	Center	-830.5
		Lowest Energy	-959.1

Cluster	Members	Representative	Weighted Score
8	28	Center	-782.6
		Lowest Energy	-1024.0
9	27	Center	-827.1
		Lowest Energy	-942.5
10	22	Center	-842.0
		Lowest Energy	-842.0
11	20	Center	-776.7
		Lowest Energy	-919.0
12	20	Center	-815.4
		Lowest Energy	-852.7
13	19	Center	-801.2
		Lowest Energy	-1015.4
14	19	Center	-808.5
		Lowest Energy	-853.5
15	18	Center	-792.6
		Lowest Energy	-897.3
16	17	Center	-773.1
		Lowest Energy	-876.2
17	17	Center	-893.6
		Lowest Energy	-893.6
18	17	Center	-796.6
		Lowest Energy	-819.2
19	16	Center	-871.3
		Lowest Energy	-941.2
20	15	Center	-784.9
		Lowest Energy	-907.1

Cluster	Members	Representative	Weighted Score
21	15	Center	-850.3
		Lowest Energy	-850.3
22	14	Center	-770.3
		Lowest Energy	-831.2
23	14	Center	-789.2
		Lowest Energy	-884.6
24	12	Center	-774.3
		Lowest Energy	-829.4
25	12	Center	-850.0
		Lowest Energy	-922.5
26	11	Center	-765.5
		Lowest Energy	-906.3
27	11	Center	-779.2
		Lowest Energy	-870.1
28	11	Center	-915.1
		Lowest Energy	-915.1
29	11	Center	-823.7
		Lowest Energy	-823.7

Table 9: *Table of results for docking with HLA receptor*

Cluster	Members	Representative	Weighted Score
0	49	Center	-962.7
		Lowest Energy	-1023.2
1	42	Center	-955.5
		Lowest Energy	-1183.6
2	39	Center	-914.8
		Lowest Energy	-1072.4
3	38	Center	-1077.4
		Lowest Energy	-1169.0

Cluster	Members	Representative	Weighted Score
4	27	Center	-1058.5
		Lowest Energy	-1058.5
5	26	Center	-1066.4
		Lowest Energy	-1232.4
6	25	Center	-1039.5
		Lowest Energy	-1061.9
7	20	Center	-1132.2
		Lowest Energy	-1132.2
8	19	Center	-1134.2
		Lowest Energy	-1134.2
9	18	Center	-1035.5
		Lowest Energy	-1035.5
10	15	Center	-1067.1
		Lowest Energy	-1067.1
11	15	Center	-992.5
		Lowest Energy	-1026.5
12	15	Center	-981.6
		Lowest Energy	-1244.9
13	14	Center	-1247.5
		Lowest Energy	-1247.5
14	14	Center	-1190.0
		Lowest Energy	-1190.0
15	13	Center	-1071.1
		Lowest Energy	-1071.1
16	13	Center	-941.0
		Lowest Energy	-1018.6
17	13	Center	-910.8
		Lowest Energy	-1108.0
18	12	Center	-1002.2
		Lowest Energy	-1002.2
19	12	Center	-1019.4

Cluster	Members	Representative	Weighted Score
		Lowest Energy	-1019.4
20	12	Center	-1006.0
		Lowest Energy	-1006.0
21	11	Center	-891.5
		Lowest Energy	-1021.8
22	11	Center	-910.6
		Lowest Energy	-976.2
23	10	Center	-913.5
		Lowest Energy	-964.2
24	10	Center	-1089.7
		Lowest Energy	-1098.9
25	10	Center	-1084.4
		Lowest Energy	-1084.4
26	10	Center	-1011.4
		Lowest Energy	-1011.4
27	10	Center	-980.1
		Lowest Energy	-980.1
28	8	Center	-892.7
		Lowest Energy	-1035.8
29	8	Center	-923.4
		Lowest Energy	-1130.0

References

Abramson J, Adler J, Dunger J, Evans R, Green T, Pritzel A, Ronneberger O, Willmore L, Ballard AJ, Bambrick J, Bodenstein SW, Evans DA, Hung C-C, O'Neill M, Reiman D, Tunyasuvunakool K, Wu Z, Žemgulytė A, Arvaniti E, Beattie C, Bertolli O, Bridgland A, Cherepanov A, Congreve M, Cowen-Rivers AI, Cowie A, Figurnov M, Fuchs FB, Gladman H, Jain R, Khan YA, Low CMR, Perlin K, Potapenko A, Savy P, Singh S, Stecula A, Thillaisundaram A, Tong C, Yakneen S, Zhong ED, Zielinski M, Žídek A, Bapst V, Kohli P, Jaderberg M, Hassabis D, Jumper JM (2024) Accurate structure prediction of biomolecular interactions with AlphaFold 3. Nature 630:493-500. 10.1038/s41586-024-07487-w

Aditi, Shariff M (2019) Nipah virus infection: A review. Epidemiol Infect 147:e95. 10.1017/s0950268819000086

Alam AM (2022) Nipah virus, an emerging zoonotic disease causing fatal encephalitis. Clin Med (Lond) 22:348-352. 10.7861/clinmed.2022-0166

Ashizawa R, Kotelnikov S, Khan O, Li SX, Glukhov E, Cao X, Lazou M, Bekar-Cesaretli A, Hailegeorgis D, Averkava V (2025) Modeling Protein–Protein and Protein–Ligand Interactions by the ClusPro Team in CASP16. Proteins: Structure, Function, and Bioinformatics

CDC (2024) Nipah virus: Facts for Clinicians. 2025:

Chan XHS, Haeusler IL, Choy BJK, Hassan MZ, Takata J, Hurst TP, Jones LM, Loganathan S, Harriss E, Dunning J, Tarning J, Carroll MW, Horby PW, Olliaro PL (2025) Therapeutics for Nipah virus disease: a systematic review to support prioritisation of drug candidates for clinical trials. The Lancet Microbe 6:10.1016/j.lanmic.2024.101002

Ching PK, de los Reyes VC, Sucaldito MN, Tayag E, Columna-Vingno AB, Malbas FF, Jr., Bolo GC, Jr., Sejvar JJ, Eagles D, Playford G, Dueger E, Kaku Y, Morikawa S, Kuroda M, Marsh GA, McCullough S, Foxwell AR (2015) Outbreak of henipavirus infection, Philippines, 2014. Emerg Infect Dis 21:328-31. 10.3201/eid2102.141433

Chua KB (2003) Nipah virus outbreak in Malaysia. Journal of Clinical Virology 26:265-275. https://doi.org/10.1016/S1386-6532(02)00268-8

Colovos C, Yeates TO (1993) Verification of protein structures: patterns of nonbonded atomic interactions. Protein Sci 2:1511-9. 10.1002/pro.5560020916

Dimitrov I, Naneva L, Doytchinova I, Bangov I (2014) AllergenFP: allergenicity prediction by descriptor fingerprints. Bioinformatics 30:846-851.

Enayatkhani M, Hasaniazad M, Faezi S, Gouklani H, Davoodian P, Ahmadi N, Einakian MA, Karmostaji A, Ahmadi K (2021) Reverse vaccinology approach to design a novel multi-epitope vaccine candidate against COVID-19: an in silico study. Journal of Biomolecular Structure and Dynamics 39:2857-2872.

Epstein JH, Field HE, Luby S, Pulliam JR, Daszak P (2006) Nipah virus: impact, origins, and causes of emergence. Curr Infect Dis Rep 8:59-65. 10.1007/s11908-006-0036-2

Garnier J (1998) GOR secondary structure prediction method version IV. Meth. Enzym., RF Doolittle Ed. 266:540-553.

Gasteiger E, Hoogland C, Gattiker A, Duvaud Se, Wilkins MR, Appel RD, Bairoch A (2005) Protein identification and analysis tools on the ExPASy server. The proteomics protocols handbook, Springer, 571-607

Goh KJ, Tan CT, Chew NK, Tan PSK, Kamarulzaman A, Sarji SA, Wong KT, Abdullah BJJ, Chua KB, Lam SK (2000) Clinical Features of Nipah Virus Encephalitis among Pig Farmers in Malaysia. New England Journal of Medicine 342:1229-1235. doi:10.1056/NEJM200004273421701

Heo L, Park H, Seok C (2013) GalaxyRefine: Protein structure refinement driven by side-chain repacking. Nucleic Acids Res 41:W384-8. 10.1093/nar/gkt458

Jespersen MC, Peters B, Nielsen M, Marcatili P (2017) BepiPred-2.0: improving sequence-based B-cell epitope prediction using conformational epitopes. Nucleic Acids Res 45:W24-w29. 10.1093/nar/gkx346

Kaushik V (2020) In silico identification of epitope-based peptide vaccine for Nipah virus. International Journal of Peptide Research and Therapeutics 26:1147-1153.

Kruiswijk C, Richard G, Salverda MLM, Hindocha P, Martin WD, De Groot AS, Van Riet E (2020) In silico identification and modification of T cell epitopes in pertussis antigens associated with tolerance. Human Vaccines & Immunotherapeutics 16:277-285. 10.1080/21645515.2019.1703453

Kumar A, Hays M, Lim F, Foster LJ, Zhou M, Zhu G, Miesner T, Hardwidge PR (2015) Protective enterotoxigenic Escherichia coli antigens in a murine intranasal challenge model. PLoS Neglected Tropical Diseases 9:e0003924.

Laskowski RA, Rullmannn JA, MacArthur MW, Kaptein R, Thornton JM (1996) AQUA and PROCHECK-NMR: programs for checking the quality of protein structures solved by NMR. J Biomol NMR 8:477-86. 10.1007/bf00228148

Lefkowitz EJ, Dempsey DM, Hendrickson RC, Orton RJ, Siddell SG, Smith DB (2017) Virus taxonomy: the database of the International Committee on Taxonomy of Viruses (ICTV). Nucleic Acids Research 46:D708-D717. 10.1093/nar/gkx932

McGuffin LJ, Bryson K, Jones DT (2000) The PSIPRED protein structure prediction server. Bioinformatics 16:404-405. 10.1093/bioinformatics/16.4.404

Mehnaz S, Anjum R, Mithila FR, Dewan SMR, Islam MR (2024) The Current Pathogenicity and Potential Risk Assessment of Nipah Virus as Potential Cause of "Disease X": A Narrative Review. Health Science Reports 7:e70241. https://doi.org/10.1002/hsr2.70241

Mire CE, Chan YP, Borisevich V, Cross RW, Yan L, Agans KN, Dang HV, Veesler D, Fenton KA, Geisbert TW, Broder CC (2020) A Cross-Reactive Humanized Monoclonal Antibody Targeting Fusion Glycoprotein Function Protects Ferrets Against Lethal Nipah Virus and Hendra Virus Infection. J Infect Dis 221:S471-s479. 10.1093/infdis/jiz515

Pettersen EF, Goddard TD, Huang CC, Meng EC, Couch GS, Croll TI, Morris JH, Ferrin TE (2021) UCSF ChimeraX: Structure visualization for researchers, educators, and developers. Protein Sci 30:70-82. 10.1002/pro.3943

Ponomarenko J, Bui HH, Li W, Fusseder N, Bourne PE, Sette A, Peters B (2008) ElliPro: a new structure-based tool for the prediction of antibody epitopes. BMC Bioinformatics 9:514. 10.1186/1471-2105-9-514

Reche PA, Glutting J-P, Zhang H, Reinherz EL (2004) Enhancement to the RANKPEP resource for the prediction of peptide binding to MHC molecules using profiles. Immunogenetics 56:405-419.

Schoch CL, Ciufo S, Domrachev M, Hotton CL, Kannan S, Khovanskaya R, Leipe D, Mcveigh R, O'Neill K, Robbertse B (2020) NCBI Taxonomy: a comprehensive update on curation, resources and tools. Database 2020:baaa062.

Sotirov S, Dimitrov I (2024) Application of machine learning algorithms for prediction of tumor T-cell immunogens. Applied Sciences 14:4034.

Spiropoulou CF (2018) Nipah Virus Outbreaks: Still Small but Extremely Lethal. The Journal of Infectious Diseases 219:1855-1857. 10.1093/infdis/jiy611

Tan CT, Goh KJ, Wong KT, Sarji SA, Chua KB, Chew NK, Murugasu P, Loh YL, Chong HT, Tan KS, Thayaparan T, Kumar S, Jusoh MR (2002) Relapsed and late-onset Nipah encephalitis. Ann Neurol 51:703-8. 10.1002/ana.10212

Tong JC, Tan TW, Ranganathan S (2007) Methods and protocols for prediction of immunogenic epitopes. Briefings in Bioinformatics 8:96-108.

Walker PJ, Siddell SG, Lefkowitz EJ, Mushegian AR, Adriaenssens EM, Alfenas-Zerbini P, Dempsey DM, Dutilh BE, García ML, Curtis Hendrickson R, Junglen S, Krupovic M, Kuhn JH, Lambert AJ, Łobocka M, Oksanen HM, Orton RJ, Robertson DL, Rubino L, Sabanadzovic S, Simmonds P, Smith DB, Suzuki N, Van Doorslaer K, Vandamme A-M, Varsani A, Zerbini FM (2022) Recent changes to virus taxonomy ratified by the International Committee on Taxonomy of Viruses (2022). Archives of Virology 167:2429-2440. 10.1007/s00705-022-05516-5

WHO (2018) Nipah Virus. 2025:

Yadav PD, Sahay RR, Balakrishnan A, Mohandas S, Radhakrishnan C, Gokhale MD, Balasubramanian R, Abraham P, Gupta N, Sugunan AP, Khobragade R, George K, Shete A, Patil S, Thankappan UP, Dighe H, Koshy J, Vijay V, Gayathri R, Kumar PJ, Rahim A, Naveen A, Nair S, Rajendran VR, Jayasree V, Majumdar T, Jain R, Viswanathan P, Patil DY, Kumar A, Nyayanit DA, Sarkale P, Waghmare A, Baradkar S, Gawande P, Bodke P, Kalele K, Yemul J, Dhaigude S, Holepannawar M, Gopale S, Chopade G, Ray S, Waghmare P, Narayan J, Mathapati B, Kadam M, Kumar A, Suryawanshi A, Jose BP, Sivadas S, Akash NP, Vimisha TV, Keerthi KV (2022) Nipah Virus Outbreak in Kerala State, India Amidst of COVID-19 Pandemic. Front Public Health 10:818545. 10.3389/fpubh.2022.818545

Zeitlin L, Cross RW, Woolsey C, West BR, Borisevich V, Agans KN, Prasad AN, Deer DJ, Stuart L, McCavitt-Malvido M (2024) Therapeutic administration of a cross-reactive mAb targeting the fusion glycoprotein of Nipah virus protects nonhuman primates. Science Translational Medicine 16:eadl2055.